

## RESEARCH ARTICLE

# Decadal shift of the influence of Arctic Oscillation on dust weather frequency in spring over the Middle East during 1974–2019

Yijie Sun<sup>1,2</sup> | Rui Mao<sup>1,2</sup>  | Dao-Yi Gong<sup>1,2</sup> | Ying Li<sup>3</sup> | Seong-Joong Kim<sup>4</sup> | Xiao-Xiao Zhang<sup>5</sup> | Xuezheng Zhang<sup>6</sup>  | Mehdi Hamidi<sup>7</sup>

<sup>1</sup>Key Laboratory of Environmental Change and Natural Disaster, Ministry of Education, Beijing Normal University, Beijing, China

<sup>2</sup>Academy of Disaster Reduction and Emergency Management, Faculty of Geographical Science, Beijing Normal University, Beijing, China

<sup>3</sup>Department of Atmospheric Science, Colorado State University, Fort Collins, Colorado, USA

<sup>4</sup>Division of Atmospheric Sciences, Korea Polar Research Institute, Incheon, South Korea

<sup>5</sup>State Key Laboratory of Desert and Oasis Ecology, Xinjiang Institute of Ecology and Geography, Chinese Academy of Sciences, Urumqi, China

<sup>6</sup>Key Laboratory of Land Surface Pattern and Simulation, Institute of Geographical Sciences and Natural Resources Research, Chinese Academy of Sciences, Beijing, China

<sup>7</sup>Faculty of Civil Engineering, Babol Noshirvani University of Technology, Babol, Iran

## Correspondence

Rui Mao, Key Laboratory of Environmental Change and Natural Disaster, Ministry of Education, Beijing Normal University, Beijing 100875, China.  
Email: mr@bnu.edu.cn

## Funding information

Key Research Program from Chinese Academy of Sciences, Grant/Award Number: ZDRW-ZS-2017-4; Korea Polar Research Institute, Grant/Award Number: PE21030; National Key R&D Program of China, Grant/Award Number: 2016YFA0602401; National Natural Science Foundation of China, Grant/Award Numbers: 41571039, 41730639, 41775068; West Light Foundation of the Chinese Academy of Sciences, Grant/Award Number: 2020-XBQNXX-015

## Abstract

Dust weather has an impact on human health and climate change in the Middle East. In this study, we examined the influence of the Arctic Oscillation (AO) on spring dust weather frequency over the Middle East at an interannual timescale during 1974–2019. The results show that there was an interdecadal shift of the influence of AO on dust weather frequency in the Middle East, with a correlation coefficient between the AO index and dust weather frequency changing from  $-0.52$  during 1974–1994 period (P1) to  $0.49$  during 1995–2013 period (P2). During P1, negative correlations between AO index and dust weather frequency were found over the northern Arabian Peninsula, and during P2, positive ones were mostly over the central and southwestern Arabian Peninsula. In the lower and middle troposphere, negative geopotential height anomalies are associated with the negative phase of the AO over South Europe during P1, whereas negative geopotential height anomalies are associated with the positive phase of the AO over Northeast Africa during P2. The negative height anomalies resulted in the occurrence of more low-pressure systems and, thus, dust weather in the Middle East. It is found that the interdecadal shift of the influence of the AO on dust weather was related to an AO-related northward displacement of wave train propagation during P2. Specifically, during P1 period, the northern branch of AO-related wave train dominated over the middle latitudes of the North Atlantic across South Europe to the Arabian Peninsula, which resulted in the negative height anomaly over South Europe in the

lower and middle troposphere. However, during P2 period, the AO-related wave train propagation moved northward, and then, the southern branch of the AO-related wave train dominated over the low latitudes of the North Atlantic across northern Africa to the Arabian Peninsula, which played an important role in the formation of the negative height anomalies over Northeast Africa.

#### KEYWORDS

Arctic Oscillation, dust weather, wave train the Middle East

## 1 | INTRODUCTION

Dust weather is one of the catastrophic weather events that has a huge impact on human health, air quality and regional climate change in the Middle East. It brings great harm to human health in the Middle East during spring (Sun *et al.*, 2016; Hamidi *et al.*, 2017; Soleimani *et al.*, 2020). It also has an effect on regional climate through direct effects of dust aerosols on solar radiation (Rezazadeh *et al.*, 2013; Jin *et al.*, 2016; Shi *et al.*, 2019; Namdari *et al.*, 2018; Jin *et al.*, 2014). Namdari *et al.* (2018) found significant relationship between dust aerosols determined by aerosol optical depth (AOD) and meteorological parameters such as rainfall and temperature on monthly time scale. Jin *et al.* (2014) showed that dust aerosols over the Arabian Sea and the Middle East are significantly correlated with the rainfall over central and eastern India about 2 weeks later. Mao *et al.* (2019) found that dust from the Middle East can be transported to the Tibetan Plateau through westerly winds in the middle troposphere, and dust deposition over the Tibetan Plateau may, in turn, magnify radiative warming in the snowpack over the Tibetan Plateau. Due to the much larger mass concentrations of dust than black carbon (Qian *et al.*, 2015), the above effect of dust on snow albedo can exceed that of black carbon on the Tibetan Plateau.

The Arctic Oscillation (AO) is the primary mode of the internal dynamics in atmospheres over the extratropical Northern Hemisphere with an equivalent barotropic structure from the surface to the lower stratosphere (Thompson and Wallace, 1998). Previous studies investigated the influence of the AO on dust storms in Northeast Asia during the spring of 1982–2006 and found that a positive AO phase not only results in decrease (increase) of dust storm frequency in Mongolia (Taklimakan Desert), but also affects dust transport in Northwest China (Gong *et al.*, 2006; Mao *et al.*, 2011a; Mao *et al.*, 2011b; Lee *et al.*, 2015; Liu *et al.*, 2020). The positive AO phase caused the northward movement of the polar jet and the strengthening of

the westerly jet over northern Tibetan Plateau. The former leads to the reduced frequency of intensive Mongolia cyclones and, thus, reduced frequency of dust storm (Mao *et al.*, 2011b).

The relationship between the AO and the climate in the Middle East has been shown in previous studies. For example, Givati and Rosenfeld (2013) and Türkes and Erlat (2008) showed that the AO exerts influence on the climate of the Middle East and its surrounding regions such as northern Indian Ocean. Gong *et al.* (2014 and 2017) demonstrated that winter AO is significantly correlated with sea surface temperature (SST) and precipitation over the western tropical Indian Ocean on the interannual time scale from 1979 to 2015. Moreover, the interdecadal change in the influence of AO on East Asian climate has been noted in several studies (Li *et al.*, 2014; Chen *et al.*, 2015). Li *et al.* (2014) documented the strengthened relationship between the East Asian winter monsoon and winter AO on the interannual time scale with a comparison of 1950–1970 and 1983–2012. The connection between AO and East Asian winter monsoon was not statistically significant during 1950–1970, but statistically significant during 1983–2012. Chen *et al.* (2015) reported that the relationship of spring AO with the following East Asian summer monsoon experienced a significant interdecadal change in the early 1970s. The influence of spring AO on the following East Asian summer monsoon is weak during the 1950s and 1960s but strong and significant during the mid-1970s through the mid-1990s.

Given the potential impact of the AO on the dust activities in the Middle East and the interdecadal shift of the relationship between the AO and East Asian winter monsoon, it is interesting to examine the possible influence of the AO on dust weather in the Middle East during recent decades, and whether there is an interdecadal change in this possible relationship. In this study, we documented the change of dust weather frequency in the Middle East in spring season during the period from 1974–2019. Then, we examined the

possible linkage between the AO and dust weather frequency in the Middle East during spring on an interannual time scale and its interdecadal changes during 1974–2019. The remainder of this paper is structured as follows: Section 2 briefly described data and research method used; Section 3 illustrated changes in the dust weather frequency and characteristics of atmospheric circulation of dust weather in the Middle East; Section 4 described the interdecadal shift of the impact of the AO on dust weather frequency in the Middle East; Sections 5 provided the possible mechanism of the interdecadal shift of AO impact and discussed whether change in the spring AO-generated sea surface temperature anomalies over the North Atlantic partly contributed to the spring AO-related atmospheric circulation anomalies around the middle East, and Section 6 was the conclusions.

## 2 | DATA AND METHOD

### 2.1 | Data

The dust data are from the global Met Office Integrated Data Archive System Land Surface Stations data (MIDAS), which are available from the British Atmospheric Data Centre (BADC) (Met Office, 2012). This dataset includes Surface Synoptic Observations (SYNOP) and Meteorological Aviation Routine Weather Report (METAR) codes every 3 or 6 hr. According to visibility, dust event records in the present weather code (ww) are classified into four types: (1) “floating dust” (ww = 6, widespread dust in suspension, not raised at or near the station at the time of observation; visibility is usually not greater than 10 km), (2) “blowing dust” (ww = 7, raised dust or sand at the time of observation, reducing visibility between 1 and 10 km), (3) “dust storm” (ww = 9 or 30–35, strong winds lift large quantities of dust particles, reducing visibility to less than 1 km), and (4) “other dust weather” (other types of dust activities are recorded in the ww code but are not related to a visibility classification) (please referencing Shao *et al.*, 2013 for details). In this study, we will focus on the analysis of two dust weather types: blowing dust and dust storm.

To analyse the changes in atmospheric circulation in association with AO variations, the Japanese 55-year Reanalysis dataset (JRA-55) was used. The JRA-55 Reanalysis dataset extends from 1958 to the present, with a horizontal resolution of  $1.25^\circ \times 1.25^\circ$  and 37 vertical levels above the surface. In this study, the variables used in the JRA-55 were geopotential height, zonal wind, meridional wind and vertical velocity in the troposphere. The AO index was obtained from the Climate Prediction Center, the National Oceanic and Atmospheric

Administration (available at [https://www.cpc.ncep.noaa.gov/products/precip/CWlink/daily\\_ao\\_index/ao.shtml](https://www.cpc.ncep.noaa.gov/products/precip/CWlink/daily_ao_index/ao.shtml)).

### 2.2 | Method

Shao *et al.* (2013) used the MIDAS data from 1974 to 2012 to analyse the trends in dust frequency and dust concentration over dust sources, including North Africa, the Middle East and Southwest Asia, Northeast Asia, South America and Australia. In this study, we will follow the method used in Shao *et al.* (2013) to analyse dust weather frequency in the Middle East ( $30^\circ\text{E}$ – $60^\circ\text{E}$   $10^\circ\text{N}$ – $35^\circ\text{N}$ ) based on the MIDAS data from 1974 to 2019 in spring (March to May). We first performed a quality check on dust records. Only dust records with good quality flags were involved in the analysis. Then, we removed those stations where days of missing records at any time were more than 30% of days in spring during 1974–2019. Finally, the remained data will be used to calculate dust weather frequency.

To present the variations in dust weather in the Middle East, we examined dust weather frequency in the Middle East. For a given spring, dust weather frequency (Fd) was defined as Equation (1), where Nd is the number of dust weather day (blowing dust or dust storm) of all stations over the research area. Noted that dust weather day at the given station was only counted as once in a given day, even though more than one dust event was recorded in a given day. Nw is the total number of stations in the selected area. Note that the number of stations in the Middle East varied during 1974–2019, which will affect the accuracy of dust weather frequency in the Middle East. In addition, dust weather frequency obtained in the year of 1977 and 1999 is not used in this study, because the data quality in these 2 years is quite low.

$$Fd = \frac{Nd}{Nw}. \quad (1)$$

Next, we examined the relationship between the AO and factors such as dust weather frequency and climatic variable on an interannual time scale. However, many previous studies showed that the climate in the Middle East may be affected by other climatic factors such as El Niño-Southern Oscillation (ENSO) and Indian Ocean Dipole (IOD) (Ashok and Saji, 2007; Niranjana Kumar *et al.*, 2016; Gong *et al.*, 2014, 2017). The impact of those climatic factors on spring dust in the Middle East may obscure the signals linked to the AO. Therefore, to highlight the impact of the AO on dust weather frequency, we have eliminated the effects of ENSO and IOD in the

study. We used Niño 3.4 index (SST anomalies in 5°N–5°S and 170°W–120°W areas) to measure ENSO. The ENSO-related components are estimated by regressing the wintertime (November–March) Niño 3.4 SST on the corresponding variables, and the non-ENSO components are estimated from the residual value of the regressions. The IOD is defined by anomalous SST gradient between the western equatorial Indian Ocean (50°E–70°E and 10°S–10°N) and the south eastern equatorial Indian Ocean (90°E–110°E and 10°S–0°N). An analogous method was used to eliminate the impact of IOD on spring dust weather. After eliminating the effects of ENSO and IOD, we confirmed the AO-related changes by a regression of climate variables against the AO time series. It should be noted that we have not considered the possible effects of the interactions between AO-IOD and AO-ENSO here (Nakamura *et al.*, 2006). After these procedures, we filtered the AO-related components of climatic factors, and only retained the components less than 10 years as the influence of the AO on the interannual time scale.

Considering that the direct factor affecting dust weather is the synoptic system, we not only focus on the relationship between AO and monthly mean of climate variables, but also analyse the relationship between AO and synoptic variability. First, we calculated the synoptic-scale disturbance to present synoptic variability. We filtered the daily data of geopotential height at 850 hPa (Mao *et al.*, 2005). As the time length of a typical weather process is about 1 week, the filtering threshold was controlled at 7 days; that is, only high-frequency changes shorter than 7 days were retained after filtering. Then, we calculated its variance as the synoptic variability.

Finally, to find out the mechanism of the interdecadal change in the relationship between AO and dust weather frequency, we used wave activity flux (Plumb, 1985) during different periods to describe quasi-stationary wave propagation. Song *et al.* (2014) and Mao *et al.* (2011c) used the analysis of wave activity flux to present the influence of AO through teleconnection. Statistical methods such as Spearman correlation and linear regression were used to study the relationship between AO index and dust weather frequency in the Middle East. Analyses were focused on the spring season (averaging from March to May) during 1974–2019.

In addition, many studies have demonstrated that North Atlantic also plays very important role in triggering spring atmospheric wave train over mid-high latitudes in Eurasia and impact Eurasian spring climate (Zhao *et al.*, 2019; Zhao *et al.*, 2020; Chen *et al.*, 2020a). A recent study also indicates that spring North Atlantic SST anomaly has a significant modulation on the ENSO-EASM relation (Chen *et al.*, 2018). Therefore, the AO-related atmospheric circulation anomalies over the

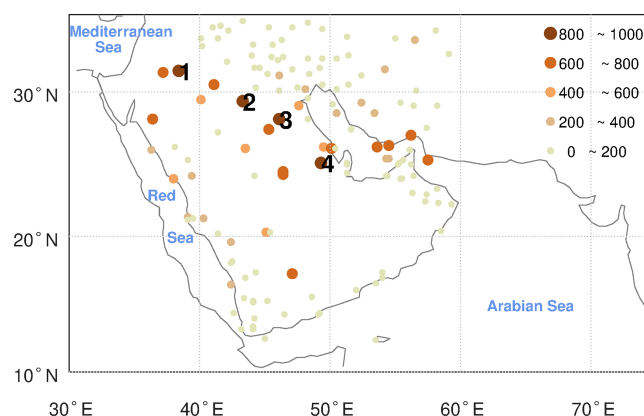
Middle East in spring may also be caused by the changes in the spring AO-generated SST anomalies over the North Atlantic. In Section 5, we examined the effect of SST in the North Atlantic on the atmospheric circulation anomalies over the Middle East. During analysis, the impact of AO as well as the ENSO and IOD on climatic variables was removed. The AO-related components were estimated by regressing the springtime AO index on the corresponding variables, and the non-AO components were estimated from the residual value of the regressions.

### 3 | DUST WEATHER IN THE MIDDLE EAST AND ITS SYNOPTIC BACKGROUND

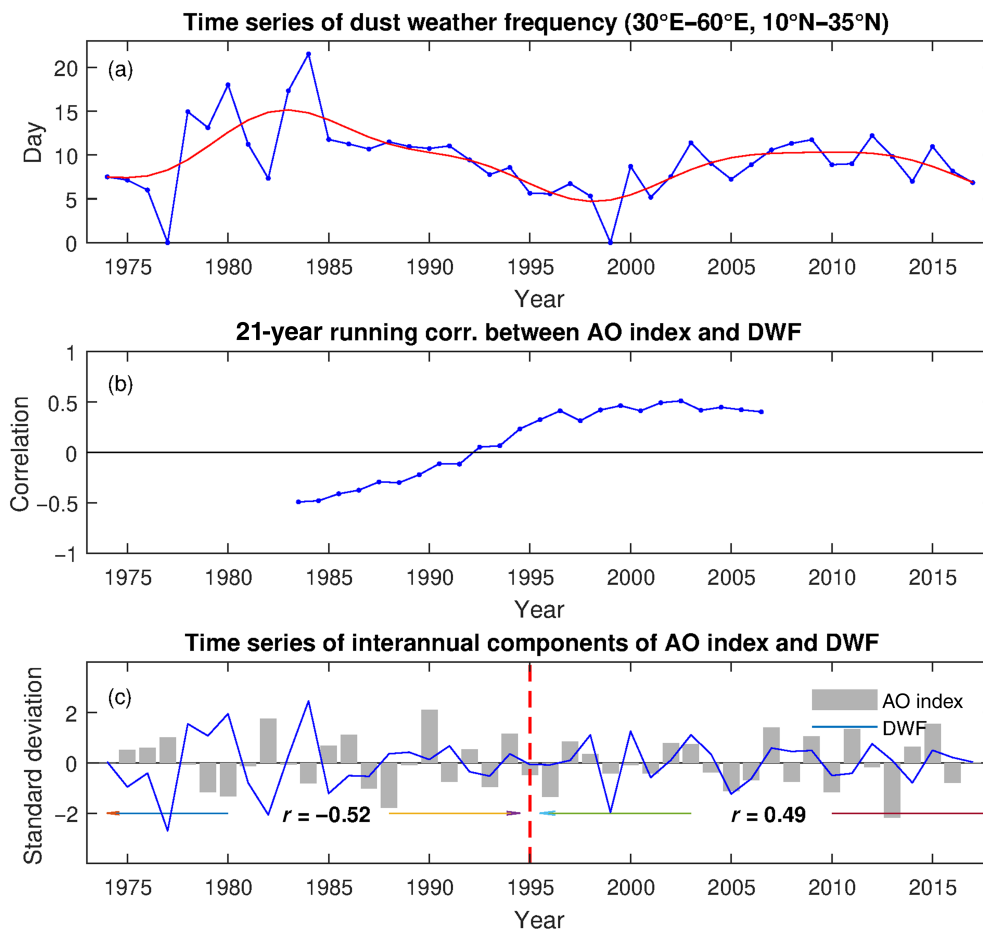
#### 3.1 | Dust weather frequency in the Middle East

Figure 1 shows the spatial distribution of days of spring-time dust weather frequency over the Middle East from 1974 to 2019. During this period, a few stations with larger days of dust weather more than 400 days are notable in the northern and eastern regions of the Arabian Peninsula and among these stations; four stations (Turaif, Rafha, Hafr Al-BatinArpt and Al Ahsa) had the total days of dust weather more than 800 days in spring during 1974–2019. In the western and southern coastal regions of the Arabian Peninsula and Iran, dust weather occurred less frequently, and the total days of dust weather were less than 200 days.

Figure 2a shows the time series of dust weather frequency in springtime from 1974 to 2019 by averaging days of dust weather over the stations in the Middle East. The average of dust weather frequency in the Middle East



**FIGURE 1** The total days of spring dust weather in the Middle East during 1974–2019 (unit: day; numbers 1–4 indicate the station of Turaif, Rafha, Hafr Al-Batin Arpt and Al ahsa, respectively) [Colour figure can be viewed at [wileyonlinelibrary.com](http://wileyonlinelibrary.com)]



**FIGURE 2** The time series of dust weather frequency (DWF) in the Middle East and its relationship with AO index. (a) The time series of DWF in the Middle East during 1974–2019 (red line indicates interdecadal component more than 10 years). (b) A 21-year sliding correlation coefficient between AO index and DWF. (c) The time series of interannual component of AO index and DWF (blue line indicates interannual component less than 10 years) [Colour figure can be viewed at [wileyonlinelibrary.com](http://wileyonlinelibrary.com)]

was 9.12 days per each spring. The dust weather frequency in the Middle East presented an interannual and interdecadal variability from 1974 to 2019 and explained 53% and 45% of the corresponding variance, respectively. The dust weather frequency increased since 1974, peaked in the middle of 1980s and decreased in 2000; afterwards, it increased from 2000 to 2010 and then decreased thereafter. Such interdecadal change of dust weather frequency was consistent with that described by Shao *et al.* (2013).

### 3.2 | Synoptic background of dust weather

The outbreak of dust weather is associated with favourable synoptic background in the lower and middle troposphere. To obtain the favourable synoptic condition for the occurrence of dust weather in the Middle East, 15 typical dust weather events were selected (see Table 1) and examined. For each event, its duration of dust weather was at least 3 days, and its visibility was less than 1 km. We then composited anomalies of geopotential height at 850 hPa level (H850) and zonal and meridional wind at 850 hPa level (UV850) (Figure 3a), geopotential height at 500 hPa

level (H500) (Figure 3b) and zonal wind at 200 hPa level (U200) (Figure 3c) during these dust weather events. For each variable, anomalies were obtained by removing the corresponding climatological-mean values during 1974–2019. Figure 3a shows a dipolar pattern of H850, with a positive anomaly over the Kazakhstan and a negative anomaly over the eastern Mediterranean. Similar dipolar pattern was also observed at 500 hPa (Figure 3b). The negative H850 anomaly over the eastern Mediterranean is associated with more frequent activities of low-pressure system, which induced southwest–northeast wind anomalies over the Middle East (Figure 3a). As shown in Barkan *et al.* (2004), the low-pressure system over Northeast Africa and the Arabian Peninsula will result in dust weather over those areas. Moreover, the negative H500 anomaly over the eastern Mediterranean implied frequent activities of troughs in the middle troposphere over the eastern Mediterranean, which result in dust weather due to the instability and wind speed at the surface in the Iraq, Syria and northern Saudi Arabia (Hamidi *et al.*, 2013; Najafi *et al.*, 2017; Hamidi, 2019).

The composite of anomalous U200 (Figure 3c) is dominated by a positive U200 anomaly, which suggests the strengthening of the jet stream orienting from the North

TABLE 1 Typical dust weather events in the Middle East

Dust weather events in the Middle East						
Date	Station name	Station code	Longitude (°E)	Latitude (°N)	Intensity of dust	Visibility (km)
March 17, 1974	Jeddah King Abdul	41024	39.1	21.4	Dust storm	0.1
March 14, 1976	Jeddah King Abdul	41024	39.1	21.4	Dust storm	0.2
April 18, 1976	Basrah Magal	40689	47.5	30.3	Dust storm	0.8
March 7, 1979	Semawa	40674	45.2	31.2	Dust storm	0.1
April 28, 1981	Dubai Intl Airport	41194	55.2	25.1	Dust storm	0.6
March 11, 1984	Bayram Ali	38895	62.1	37.4	Dust storm	0.6
March 19, 1985	Riyadh King Khalid	40437	46.4	24.6	Dust storm	0.4
March 9, 1989	Hafr Al-Batin Arpt	40373	46.1	28.2	Dust storm	0.3
April 8, 1991	King Khalid Mil Cty	40377	45.3	27.5	Dust storm	0.2
May 19, 1991	Hafr Al-Batin Arpt	40373	46.1	28.2	Dust storm	0.1
March 18, 1998	Kzyl-Orda	38062	65.3	44.5	Dust storm	0.2
March 20, 2002	Kzyl-Orda	38062	65.3	44.5	Dust storm	0.3
March 12, 2003	Kuwait Intl Arpt	40582	47.6	29.1	Dust storm	0.1
April 24, 2006	Hafr Al-Batin Arpt	40373	46.1	28.2	Dust storm	0.1
March 26, 2008	Turaif	40356	38.4	31.4	Dust storm	0.1

Africa to northern Arabian Peninsula. Duan *et al.* (2013) indicated that the initiation of dust storm in East Asia was related to the enhancement of westerly jet, which promoted the formation of cyclones in the lower troposphere to the north of the exit region of the westerly jet. Therefore, we argue that the enhanced westerly jet over the North Africa and the northern Arabian Peninsula played an important role in initiating dust weather at the surface through increased cyclone activities.

## 4 | THE INTERDECADAL SHIFT OF THE INFLUENCE OF AO ON DUST WEATHER FREQUENCY

### 4.1 | The interdecadal shift of relationship between AO index and dust weather frequency

Figure 2b shows a 21-year sliding correlation coefficient between dust weather frequency in the Middle East and AO index during spring with a period of 1974–2019. It is very clear that the 21-year sliding correlation coefficient has an interdecadal variation, changing from negative correlation before 1995 to positive correlation afterwards. Before 1995, the negative correlation continually decreased to zero in 1994. Thereafter, the sliding correlation coefficient continued to increase and reached a peak in 2001. After 2001, the positive correlation coefficient decreased slightly. Thus, we split the study period into two subperiods, that is, 1974–1994

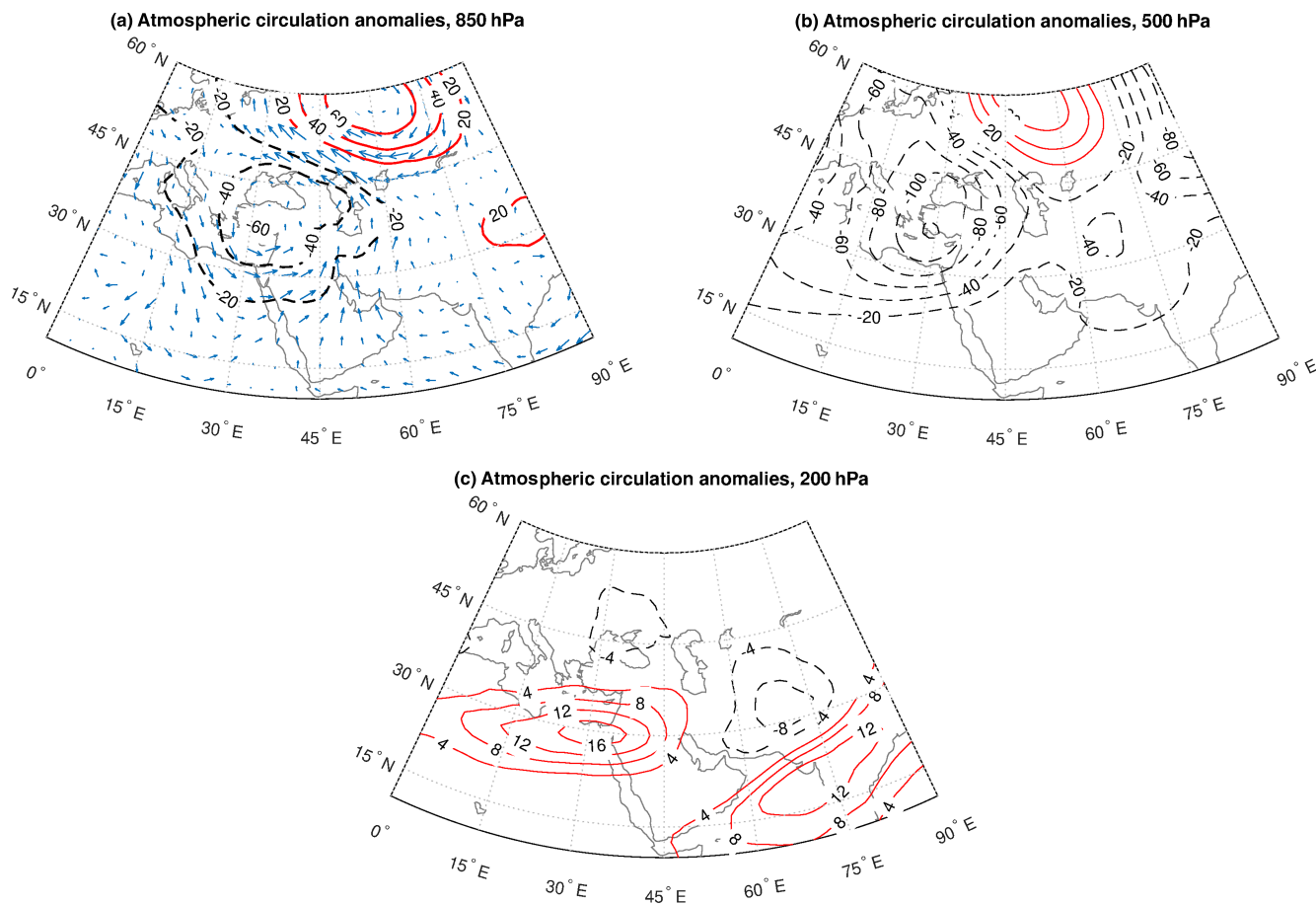
(P1) and 1995–2013 (P2) and calculated the correlation coefficient between the AO index and dust weather frequency in spring for these two subperiods (Figure 2c). The correlation was  $-0.52$  in P1 and  $0.49$  in P2, which were significant at the 95% confidence level.

Figure 4 shows the spatial distribution of stations with correlation coefficients between AO index and dust weather frequency in spring during two subperiods. During P1 period, there was a large area of negative-correlation stations over the central part of the northern Arabian Peninsula from the Red Sea to the Persian Gulf. However, there were positive-correlation stations over the central and southern Arabian Peninsula during P2 period. Although the correlation coefficient at stations is insignificant because of a low freedom degree in the correlation analysis, a large number of stations showing homogeneous correlation coefficients during P1 and P2 indicates that AO has a unified effect on dust weather frequency at the spatial scale. These results further indicated that AO had a negative (positive) correlation with dust weather frequency during P1 (P2) period over the Arabian Peninsula.

### 4.2 | Changes in atmospheric circulation related to AO variations during P1 and P2

#### 4.2.1 | Changes in synoptic variance

According to the sliding correlation analysis, there was an interdecadal shift of the relationship between dust



**FIGURE 3** Anomalies of atmospheric circulation in association with dust weather at (a) 850 hPa, (b) 500 hPa and (c) 200 hPa. In (a,b), the geopotential height was depicted by contours, and wind field was indicated by arrows. In (c), the zonal wind was depicted by contours. Units: gpm for geopotential height and  $\text{m}\cdot\text{s}^{-1}$  for winds. Positive and negative values are indicated by solid lines and dashed lines, respectively. The zero contours are omitted for clarity [Colour figure can be viewed at [wileyonlinelibrary.com](http://wileyonlinelibrary.com)]

weather frequency and AO index over the Arabian Peninsula from P1 to P2. Therefore, we compared the changes in atmospheric circulation in association with AO variations in spring during P1 and P2 periods. The results show that when the AO was at the negative phase, there was a positive anomaly over the Mediterranean Sea and Northeast Africa and a large area of negative anomaly over the central European region (Figure 5). These anomalies are significant at the 95% confidence level. It means that during the P1 period, the atmosphere circulation over the Mediterranean region and North Africa had strong disturbance, which triggered the occurrence of dust weather over Northeast Africa and, therefore, induced dust weather over the Middle East through dust transport. During the P2 period, there was a negative anomaly of synoptic-scale variability over the Mediterranean region and a positive anomaly in the eastern and southern parts of the Middle East. This shows that when the AO was at the positive phase, the circulation over the eastern and southern Middle East has large variability

and strong disturbance at the synoptic scale, resulting in the dust weather in the Middle East. By comparing the changes of two periods, we know that the negative phase of the AO is likely to influence dust weather occurrence from Northeast Africa to the Middle East in P1 period. In the P2 period, the positive phase of the AO has a stronger influence on the eastern and southern Middle East, which leads to the dust weather.

#### 4.2.2 | Changes in UV850, H850 and H500

During P1 period, when AO was in a negative phase, there was a large area of positive H850 anomaly in the middle- to high-latitude from Europe to Siberia and a negative H850 anomaly over southern Europe and the Mediterranean (Figure 6a). These H850 anomalies were significant at the 95% confidence level. The negative H850 anomaly over the south Europe and the Mediterranean implied frequent low-pressure activities over the

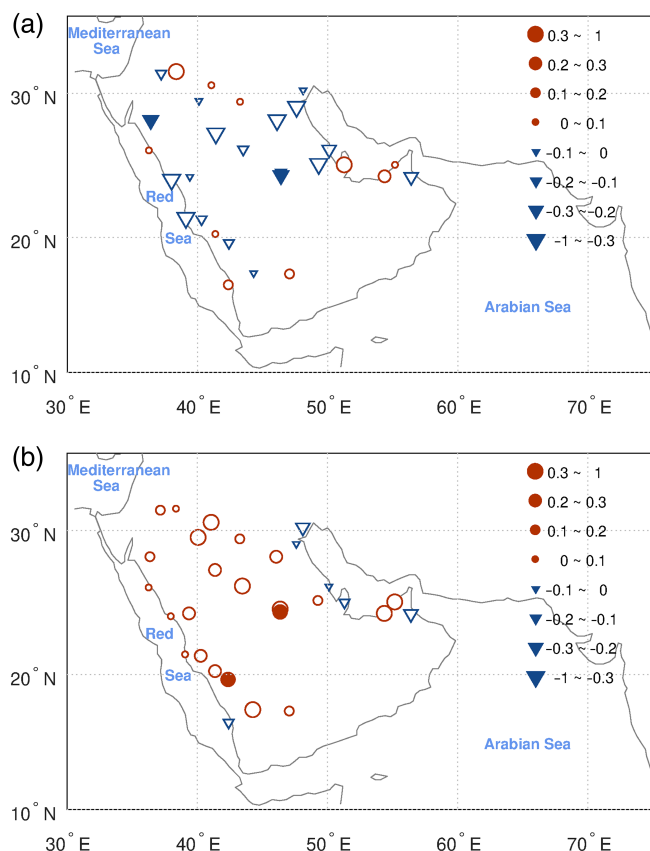


**FIGURE 4** The correlation coefficient between spring dust weather frequency and AO index during (a) 1974–1994 and (b) 1995–2013. The red dot indicates positive correlation, and downward triangle indicates negative correlation. Significant at 95% confidence level is filled [Colour figure can be viewed at [wileyonlinelibrary.com](http://wileyonlinelibrary.com)]

Mediterranean, as shown in Figure 3a. The airflows of southwest–northeast direction of low-pressure activities caused increased wind speed at the surface and led to dust weather in Northeast Africa (Hamidi *et al.*, 2013; Najafi *et al.*, 2017; Hamidi, 2019; Mao *et al.*, 2019). Subsequently, the northern Arabian Peninsula was affected by dust transported from North Africa, resulting in more dust weather over there (Mao *et al.*, 2019). The regressions of H500 against the AO index show a similar pattern of those of 850 hPa during P1 period, that is, negative height anomalies over the south Europe and positive height anomalies over northern Europe and Northeast Africa (Figure 7a). The negative height anomalies over the south Europe and the positive height anomalies over Northeast Africa induced southwesterly winds from Northeast Africa to the northern Arabian Peninsula and hence dust weather over the northern Arabian Peninsula (Hamidi *et al.*, 2013; Hamidi, 2019; Mao *et al.*, 2019).

During P2, the regressions of H850 against the AO index show similar patterns during P2 (Figure 6b). When

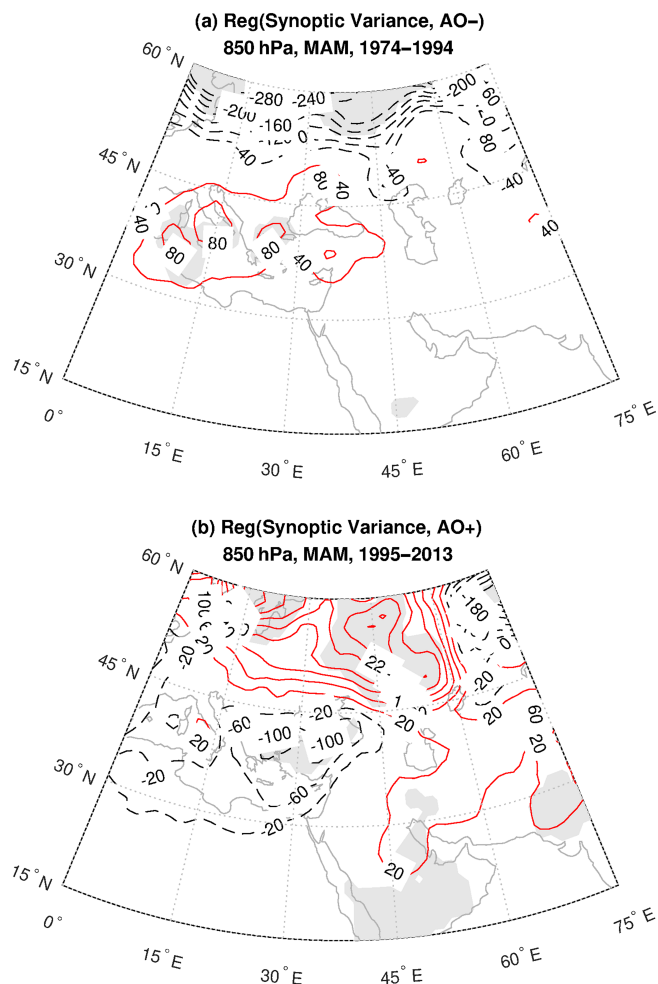


**FIGURE 5** The regression coefficient of synoptic variance by the AO index during (a) 1974–1994 and (b) 1995–2013. Significant at 95% confidence level is shaded. The synoptic variance was depicted by contours. Units:  $\text{gpm}^2$ . Positive and negative values are indicated by solid lines and dashed lines, respectively. The zero contours are omitted for clarity [Colour figure can be viewed at [wileyonlinelibrary.com](http://wileyonlinelibrary.com)]

AO was in a positive phase, H850 anomalies showed a strong positive height anomaly over Europe and a weak positive height anomaly over Mongolia. In the meantime, there were negative H850 anomalies over northern Africa and between two positive anomalies of Europe and Mongolia. The regressions of H500 during P2 show a pattern as well as that for H850, with positive anomalies over Europe and Siberia and negative anomalies stretching from northern Africa across northern Arabian Peninsula to the Middle Asia (Figure 7b). The negative H850/H500 anomaly over Northeast Africa and northern Arabian Peninsula played a role in the increase of dust weather frequency over the Arabian Peninsula during P2 for the positive AO phase. By comparing the regressions

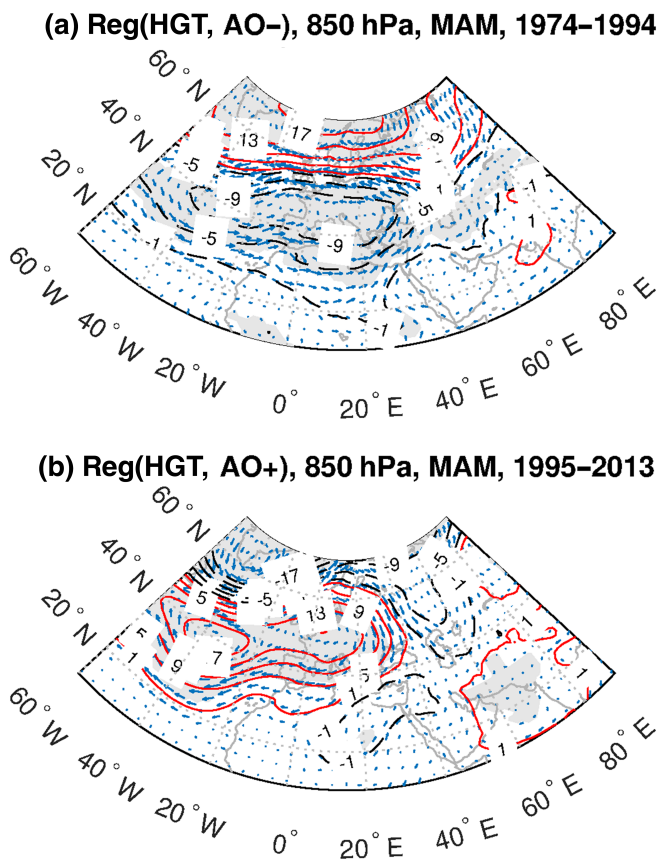


**FIGURE 6** The regression coefficient of geopotential height at 850 hPa regressed by the AO index during a) 1974–1994 and b) 1995–2013. Significant at 95% confidence level is shaded. The geopotential height was depicted by contours, and wind field was indicated by arrows. Units: gpm for geopotential height and  $\text{m}\cdot\text{s}^{-1}$  for winds. Positive and negative values are indicated by solid lines and dashed lines, respectively. The zero contours are omitted for clarity [Colour figure can be viewed at [wileyonlinelibrary.com](http://wileyonlinelibrary.com)]

of H850/H500 during P1 and P2 periods, the negative height anomaly over the Mediterranean moved southward to Northeast Africa from P1 to P2. It means that the location of low-pressure systems over the Mediterranean may be displaced southward in P2 away from that in P1, which explained more stations showing high correlation along the southwestern coast of the Arabian Peninsula during P2, as shown in Figure 4.

#### 4.2.3 | Changes in U200

The regression of U200 against the AO index during P1 period shows positive U200 anomalies over the Mediterranean and negative U200 anomalies over the northern Europe and the northern Africa (Figure 8a). Compared with the location of westerly jet axis during P1 period, the positive U200 anomalies over the Mediterranean indicated a northward displacement of westerly jet axis and

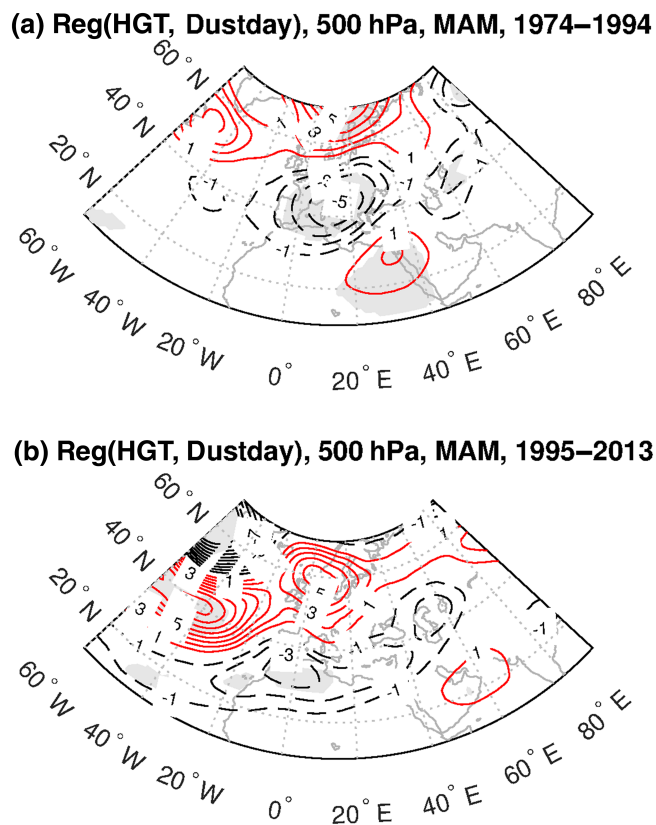


**FIGURE 7** The regression coefficient of geopotential height at 500 hPa regressed by the AO index during a) 1974–1994 and b) 1995–2013. Significant at 95% confidence level is shaded. The geopotential height was depicted by contours. Units: gpm for geopotential height. Positive and negative values are indicated by solid lines and dashed lines, respectively. The zero contours are omitted for clarity [Colour figure can be viewed at [wileyonlinelibrary.com](http://wileyonlinelibrary.com)]

enhanced westerly jet during P1 when AO was in a negative phase. The northward westerly jet was conducive to dust weather, because westerly jet caused a downward momentum transfer and then benefited the development of dust events over Northeast Africa (Mao *et al.*, 2019). In the meantime, because of the secondary flow of westerly jet in the troposphere in the entrance region of westerly jet, uplift air flows in the middle to high troposphere between  $27.5^{\circ}\text{N}$  and  $40^{\circ}\text{N}$  played an important role in pumping dust into the free atmosphere over the Northeast Africa and the northern Arabian Peninsula (Figure 9a).

During P2, when AO was in a positive phase, there was a positive U200 anomaly orienting from northern Africa to the Middle East. In the meantime, there was a large area of negative U200 over southern Europe and the Mediterranean. The positive U200 anomalies over the northern Africa were located over the location of climatological westerly jet axis during P2, indicating an enhanced westerly jet over Northeast Africa during P2

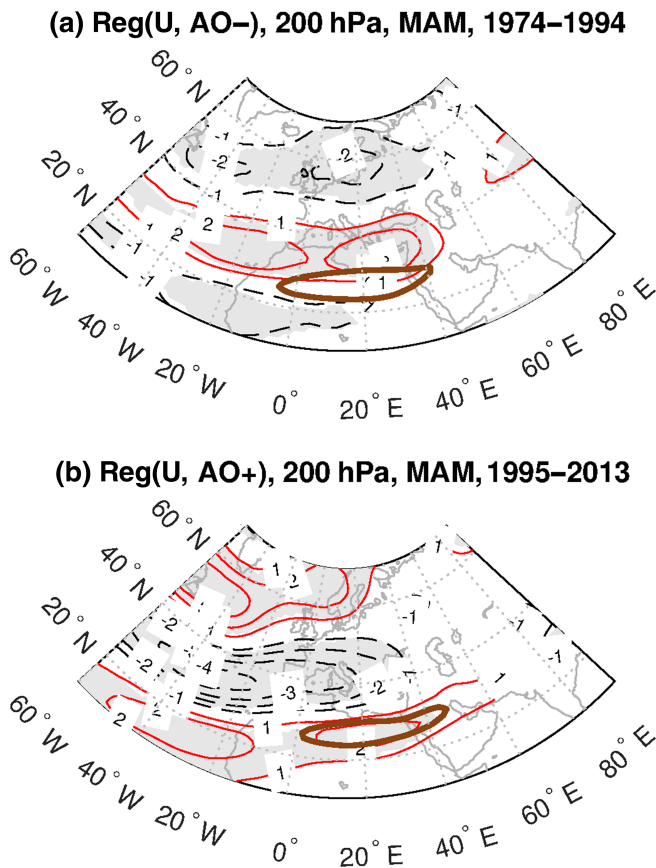


**FIGURE 8** The regression coefficient of zonal wind at 200 hPa regressed by the AO index during a) 1974–1994 and b) 1995–2013. The brown line indicates the jet core with a wind speed of  $40 \text{ m}\cdot\text{s}^{-1}$ . Significant at 95% confidence level is shaded. The zonal wind was depicted by contours. Units:  $\text{m}\cdot\text{s}^{-1}$ . Positive and negative values are indicated by solid lines and dashed lines, respectively. The zero contours are omitted for clarity [Colour figure can be viewed at [wileyonlinelibrary.com](http://wileyonlinelibrary.com)]

period when AO was in the positive phase. The increased westerly jet was helpful for dust weather occurrence as depicted in Figure 3c. The westerly jet caused a downward momentum transfer and uplift air flows between  $20^\circ\text{N}$  and  $35^\circ\text{N}$  in the middle to high troposphere induced by the secondary flow of westerly jet in its entrance region (Figure 9b).

Compared with the regression of U200 in P1, the positive U200 anomaly in P2 was located southward and eastward. The southward and eastward movement of positive U200 anomaly was consistent to the southward and eastward displacement of negative H500/H850 anomaly over the Mediterranean in the lower to middle troposphere from P1 to P2. The southward and eastward displacement of low-pressure systems and westerly jet resulted in the increased influence of AO on dust weather frequency over southwestern Arabian Peninsula during P2, indicated by increased synoptic variance over the Middle East

(Figure 5b), southward displacement of anomalous updrafts and more high-correlation stations along the southeast coast of the Arabian Peninsula during P2 than P1 (Figures 4 and 9).

## 5 | DISCUSSIONS

### 5.1 | Mechanism of the interdecadal shift of the influence of AO on dust weather frequency

To examine the AO-related teleconnection pattern, following Song *et al.* (2014), the regressions of meridional wind at 300 hPa level (V300) against AO index during P1 and P2 were analysed. In general, the regressions of V300 revealed that the AO-related wave train propagated eastward and equatorward from the mid-latitudes of the North Atlantic during P1 and P2 (Figure 10). Besides the wave train propagated equatorward from mid-latitude to low-latitude over North Atlantic, there was a northern branch and a southern branch of wave train from the mid-latitude of North Atlantic to downstream regions over Eurasia. During P1 period, the northern branch stretched from the mid-latitude of North Atlantic, eastern Europe and the Arabian Peninsula; the southern branch was displayed with centres from the low-latitudes of North Atlantic across northern Africa to the Arabian Peninsula. Compared with P1 period, the propagation of northern branch of wave train became stronger and more northward during P2, propagating from the mid-latitude of North Atlantic across Europe to the Siberia. In the meantime, the southern branch of wave train continued to spread eastward, affecting North Africa with a positive (negative) anomaly over Northwest (Northeast) Africa. According to the anomalous low-pressure system in the regressions of H500/H850 shown in Figures 6 and 7, it concludes that the anomalous low-pressure system in the P1 period was possibly caused by the northern branch of wave train. However, the southern branch of wave train may play a role in the formation of the anomalous low-pressure system over the Northeast Africa during P2 period.

For a clear depiction of the different propagation directions of the AO-related wave trains, quasi-stationary wave-activity fluxes (vectors), defined by Plumb (1985), during the P1 and P2 were also shown in Figure 11. There were two wave trains from North Africa to downstream regions revealed by wave activity fluxes as well as the results of V300. Besides the equatorward propagation of wave train over North Atlantic from middle latitudes to low latitudes, the northern wave train mainly stretched from Europe across the eastern Mediterranean to the Arabian Peninsula. In the meantime, the southern

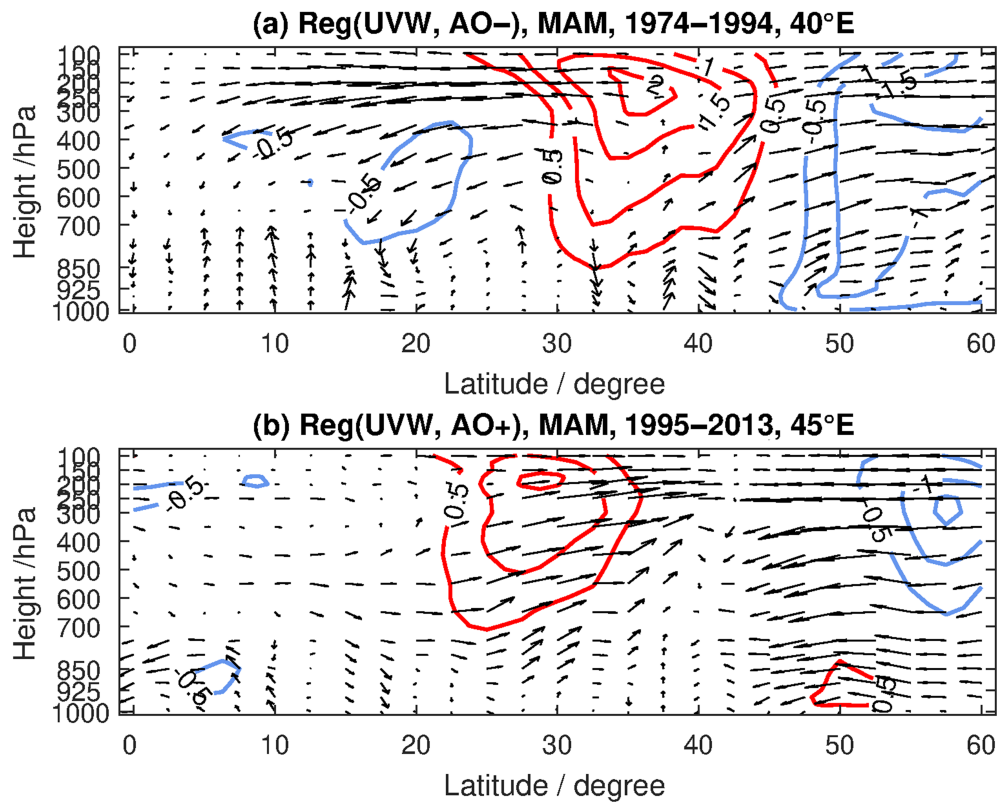


FIGURE 9 Vertical profiles of regression coefficients of wind fields along (a) 40°E and (b) 45°E against the AO index. Contour lines denote zonal wind (in  $\text{m}\cdot\text{s}^{-1}$ ), and arrows denote meridional (in  $\text{m}\cdot\text{s}^{-1}$ ) and vertical velocity (in  $\text{pa}\cdot\text{s}^{-1}$ ). For demonstration, vertical velocity is multiplied by 200 [Colour figure can be viewed at [wileyonlinelibrary.com](http://wileyonlinelibrary.com)]

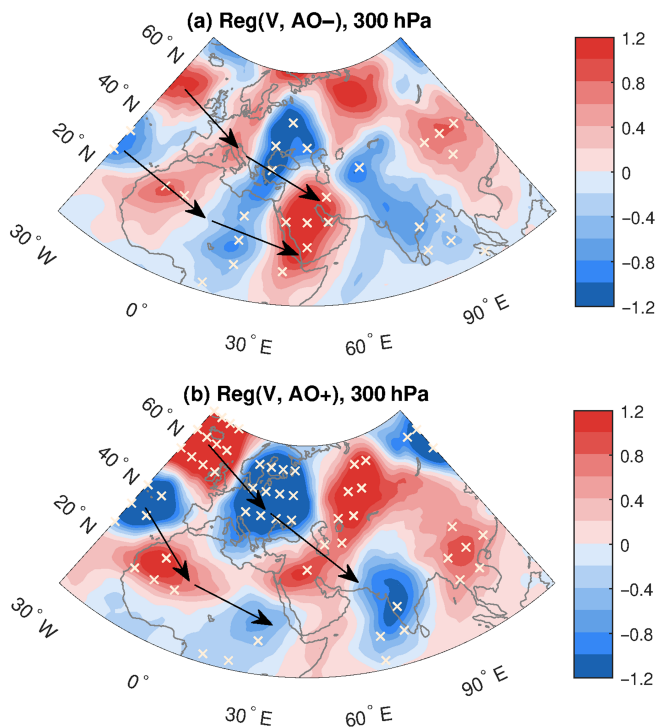


FIGURE 10 The regression coefficient of meridional wind at 300 hPa level regressed by the AO index during (a) 1974–1994 and (b) 1995–2013. Units:  $\text{m}\cdot\text{s}^{-1}$ ; red/blue contours represent positive/negative values. The heavy arrows superimposed on the figure show the pathway of the northern and southern branch of the AO-related wave train [Colour figure can be viewed at [wileyonlinelibrary.com](http://wileyonlinelibrary.com)]

wave train also transported from the low-latitude of the North Atlantic to the North Africa during P1. However, the two branches of wave train moved more northward during P2 than P1. As a result, the southern one played a role in the formation of the anomalous low-pressure system over Northeast Africa during P2.

By comparing the vertical wave activity fluxes between P1 and P2, the positive value in the mid-latitude of North Atlantic, as a possible source of wave activity, was higher during P2 than P1. It means that the wave activity fluxes were strengthened during P2 than P1. We speculated that the northern and southern branch of wave activity over the North Atlantic may be stronger during P2 than P1.

## 5.2 | Possible causes of the AO-related northward displacement of wave train propagation during P2 period

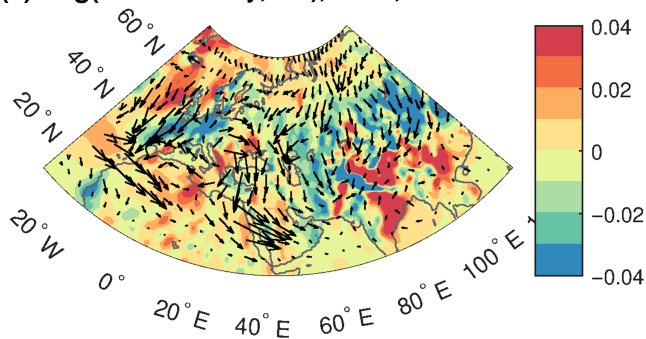
We intended to understand the causes of the interdecadal northward wave train propagation during P2 period in association with AO variations. Gao *et al.* (2014) reported that there was an interdecadal change in the relationship between springtime AO and East Asian summer monsoon in late 1990s, which was caused by large differences in the AO pattern between 1979–1997 and 1998–2007. In pre-1997, the spring AO-associated wave activity prefers the high-latitude propagation from North Atlantic to

Pacific. In contrast, a subtropical wave train from North Atlantic Ocean to Indian Ocean is evidently enhanced in post-1997 epoch. Therefore, we compared the spring AO

pattern before 1995 with that after 1995 at the inter-annual timescale (Figure S1).

The AO pattern before 1995 presented weak anomalies over northern Atlantic Ocean and strong ones over the northern Pacific Ocean. Reversely, the AO pattern after 1995 was featured by strong anomalies over the northern Atlantic Ocean and weak ones over the Pacific Ocean. Therefore, we thought that the AO-related northward displacement of wave train propagation after 1995 may be related to the strengthening signals of spring AO over North Atlantic Ocean. The mechanisms of why different spring AO pattern induced different wave train propagations in the middle latitudes will be addressed in future works.

**(a) Reg(wave-activity, AO), MAM, 1974–1994**



**(b) Reg(wave-activity, AO), MAM, 1995–2013**

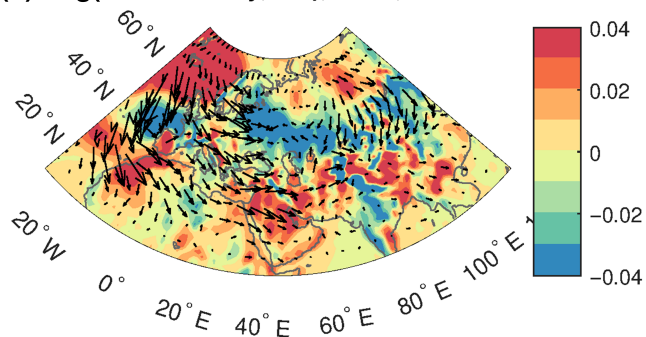


**FIGURE 11** Regression coefficients of wave activity flux against the AO index during (a) 1974–1994 and (b) 1995–2013. The regression coefficients of horizontal wave activity flux are vertically averaged from 300 to 500 hPa (arrows,  $m^2 \cdot s^{-2}$ ), and vertical wave activity flux is vertically averaged from 1,000 to 850 hPa (shaded,  $m^2 \cdot s^{-2}$ ) [Colour figure can be viewed at wileyonlinelibrary.com]

### 5.3 | The influence of North Atlantic SST on the atmospheric circulation anomalies

Some previous studies indicated that the North Atlantic Ocean may have a certain effect on Eurasian climate through atmospheric wave trains (e.g., Wu *et al.*, 2009; Zuo *et al.*, 2013; Chen *et al.*, 2018; Chen *et al.*, 2020a, 2020b). For example, a tripole SST anomaly pattern in the North Atlantic Ocean features a wave pattern over the North Atlantic and Eurasia and, hence, influences Eurasian spring climate and even the East Asian summer monsoon (Wu *et al.*, 2009). Therefore, we wonder whether the spring AO-related atmospheric circulation anomalies around the middle East may be partly due to changes in the spring AO-generated SST anomalies over the North Atlantic.

We first examined the regression of North Atlantic SST against AO index during 1974–1994 (P1) and 1995–2013

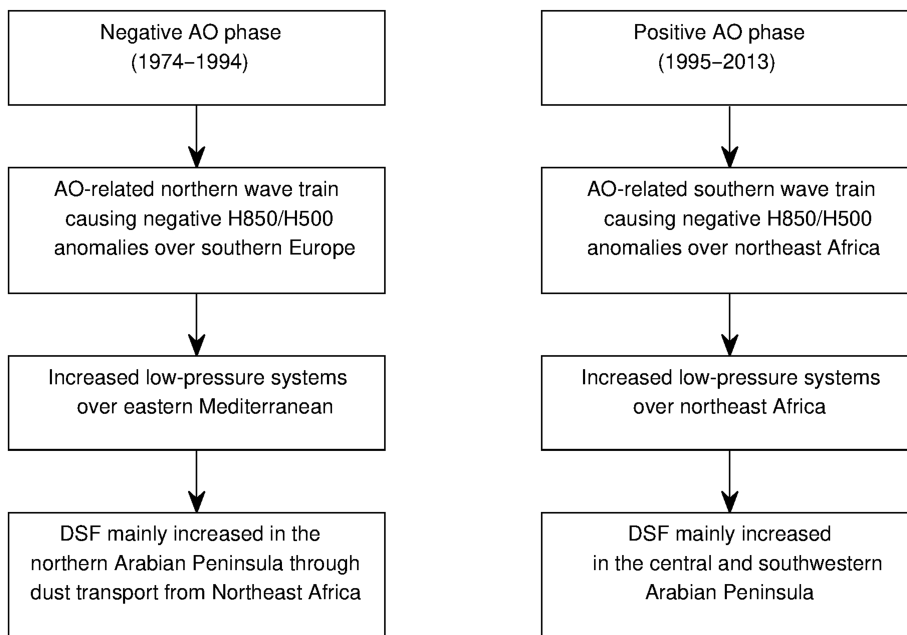


**FIGURE 12** The processes of how AO influences dust weather frequency in the Middle East

(P2), respectively (Figure S2). The results show that the AO had a close relationship with North Atlantic tripole SST (NAT) pattern during boreal spring. To examine the role of NAT in inducing atmospheric circulation anomalies, we examined the regressions of H850/H500 against the NAT index (NATI). The NATI index was defined as the regional average of the mid-latitudes of the North Atlantic Ocean ( $28^{\circ}$ – $36^{\circ}$ N,  $40^{\circ}$ – $74^{\circ}$ W) minus half of the sum of the regional average of the high latitudes ( $46^{\circ}$ – $60^{\circ}$ N,  $26^{\circ}$ – $50^{\circ}$ W) and the regional average of the low latitudes ( $2^{\circ}$ – $22^{\circ}$ N,  $18^{\circ}$ – $58^{\circ}$ W) (Li *et al.*, 2019). During analysis, the impact of AO as well as the ENSO and IOD on H850/H500 was removed to highlight the pure effect of NAT.

During the P1 period, when AO was in the negative phase, the NAT was in a negative phase, that is, two positive anomalies in the northern and southern of the North Atlantic and one negative anomaly in the central part of North Atlantic. Accordingly, the negative NAT phase was related to a positive H850 and H500 anomaly over the Mediterranean and a negative one over the Ural Mountains (Figures S3a and S4a). The positive height anomalies in the lower to middle troposphere over the eastern Mediterranean were not helpful for the formation of low-pressure systems over there, which may reduce dust weather occurrence over the Middle East. Similarly, in the P2 period (Figures S3b and S4b), when AO was in a positive phase, the NAT was in a positive phase, that is, two negative anomalies in the northern and southern of the North Atlantic and one positive anomaly in the central part of North Atlantic. The positive NAT phase was related to a weak influence over the eastern Mediterranean and the Middle East at 850 hPa and a positive height anomaly over the Middle East at 500 hPa. It is evident that the positive height anomaly over the Middle East in the middle troposphere was not helpful for dust weather occurrence. Based on the results above, we thought that the spring AO-generated SST anomalies over the North Atlantic may not contribute to the spring AO-related atmospheric circulation anomalies around the middle East. This conclusion was supported by Chen *et al.* (2020a, 2020b) and Chen *et al.* (2006) that the North Atlantic SST anomalies play an important role in the maintenance of the spring atmospheric wave train in the middle latitudes other than low latitudes. In summary, changes in AO were a major factor in the interdecadal shift of the interannual relationship between AO and dust weather over the Middle East.

## 6 | CONCLUSION

Based on MIDAS data and the JRA-55 Reanalysis data, we analysed changes in the dust weather over the Middle

East and their relationship with AO during 1974–2019 (Figure 12). There was an interdecadal change in the relationship between AO and dust weather frequency over the Middle East, with a negative correlation before 1995 and a positive one afterwards; the correlation coefficient between AO index and dust weather frequency in the Middle East was  $-0.52$  and  $0.49$ , respectively, during 1974–1994 (P1) and 1995–2013 (P2) period. During P1 period, when AO was in a negative phase, there was an increased synoptic variance in the lower troposphere, a negative H850/H500 anomaly and an enhanced westerly jet over the Mediterranean. As a result, stations over the northern Arabian Peninsula from the Red Sea to the Persian Gulf showed increased dust weather frequency. During P2 period, when AO was in a positive phase, the synoptic variance increased over the Middle East. In the meantime, anomalous negative H850/H500 moved southward over Northeast Africa and westerly jet increased over Northeast Africa and the northern Arabian Peninsula. At this condition, dust weather frequency increased over the central and southern Arabian Peninsula during P2.

The reason for the interdecadal shift of the influence of AO on dust weather was related to changes in wave train propagation corresponding to AO variations from 1974 to 2019. The AO-related wave trains were divided into two branches: the northern branch stretching from the mid-latitudes of North Atlantic across South Europe to the Arabian Peninsula and the southern one extending from the low-latitudes of North Atlantic across North Africa to the Arabian Peninsula. During P1 period, the northern branch of wave train dominated the negative H850/H500 anomaly over South Europe. During P2 period, the south branch of wave train played a role in the formation of the negative H850/H500 anomaly over Northeast Africa, causing dust weather occurring more southward during P2 than P1.

## ACKNOWLEDGEMENTS

The authors thank Prof. Yaping Shao and Dr. Martina Klose for analysing the dust observations from the global Met Office Integrated Data Archive System, UK Meteorological Office. This research was supported by the National Key R&D Program of China (2016YFA0602401). Rui Mao was supported by the National Natural Science Foundation of China (41571039, 41730639), Key Research Program from CAS (ZDRW-ZS-2017-4) and Project PE21030 of the Korea Polar Research Institute. Gong DY was supported by the NSFC-41775068. Zhang XX was supported by the West Light Foundation of the Chinese Academy of Sciences (no. 2020-XBQNXZ-015).

## AUTHOR CONTRIBUTIONS

**Yijie Sun:** Data curation; formal analysis; investigation; methodology; software; visualization; writing – original draft; writing – review and editing. **Rui Mao:** Conceptualization; methodology; project administration; resources; supervision; writing – review and editing. **Gong Dao-Yi:** Conceptualization; supervision. **Ying Li:** Conceptualization; writing – original draft; writing – review and editing. **Seong-Joong Kim:** Conceptualization; writing – original draft. **Xiaoxiao Zhang:** Conceptualization; writing – original draft. **xuezhen zhang:** Conceptualization; formal analysis. **Mehdi Hamidi:** Conceptualization; resources.

## ORCID

Rui Mao  <https://orcid.org/0000-0003-1310-0839>

Xuezhen Zhang  <https://orcid.org/0000-0002-3845-2403>

## REFERENCES

- Ashok, K. and Saji, N.H. (2007) On the impacts of ENSO and Indian Ocean dipole events on sub-regional Indian summer monsoon rainfall. *Natural Hazards*, 42, 273–285.
- Barkan, J., Kutiel, H. and Alpert, P. (2004) Climatology of dust sources in North Africa and the Arabian Peninsula, based on TOMS data. *Indoor and Built Environment*, 13(6), 407–419.
- Chen, S., Wu, R. and Chen, W. (2018) Modulation of spring northern tropical Atlantic sea surface temperature on the El Niño–Southern Oscillation–East Asian summer monsoon connection. *International Journal of Climatology*, 38, 5020–5029.
- Chen, S., Wu, R. and Chen, W. (2020b) Strengthened connection between springtime North Atlantic Oscillation and North Atlantic tripole SST pattern since the late-1980s. *Journal of Climate*, 35(5), 2007–2022.
- Chen, S., Wu, R., Chen, W., Hu, K. and Yu, B. (2020a) Structure and dynamics of a springtime atmospheric wave train over the North Atlantic and Eurasia. *Climate Dynamics*, 54, 5111–5126.
- Chen, S.F., Chen, W. and Wu, R. (2015) An interdecadal change in the relationship between boreal spring Arctic Oscillation and the East Asian summer monsoon around the early 1970s. *Journal of Climate*, 28, 1527–1542.
- Chen, W., Kang, L.H. and Wang, D. (2006) The coupling relationship between summer rainfall in China and global sea surface temperature. *Climatic and Environmental Research (in Chinese)*, 11(3), 259–269.
- Duan, H.X., Li, Y.H., Pu, C.X., Zhao, J.H. and Zhang, L. (2013) The influence of high level jet on dust transportation in a sandstorm process. *Journal of Desert Research*, 33(05), 1461–1472.
- Gao, M.N., Yang, J., Gong, D.Y. and Kim, S.J. (2014) Unstable relationship between spring Arctic Oscillation and East Asian summer monsoon. *International Journal of Climatology*, 34, 2522–2528.
- Givati, A. and Rosenfeld, D. (2013) The Arctic Oscillation, climate change and the effects on precipitation in Israel. *Atmospheric Research*, s132–133, 114–124.
- Gong, D.Y., Gao, Y.Q., Guo, D., Mao, R. and Gao, M.N. (2014) Interannual linkage between Arctic/North Atlantic Oscillation and tropical Indian Ocean precipitation during boreal winter. *Climate Dynamics*, 42, 1007–1027.
- Gong, D.Y., Guo, D., Gao, Y.Q., Yang, J. and Kim, S.J. (2017) Boreal winter Arctic Oscillation as an indicator of summer SST anomalies over the western tropical Indian Ocean. *Climate Dynamics*, 48, 2471–2488.
- Gong, D.Y., Mao, R. and Fan, Y.D. (2006) East Asian dust storm and weather disturbance: possible links to the Arctic Oscillation. *International Journal of Climatology*, 26, 1379–1396.
- Hamidi, M. (2019) Atmospheric investigation of frontal dust storms in Southwest Asia. *Asia-Pacific Journal of Atmospheric Sciences*, 55, 177–193.
- Hamidi, M., Kavianpour, M.R. and Shao, Y.P. (2013) Synoptic analysis of dust storms in the Middle East. *Asia-Pacific Journal of Atmospheric Sciences*, 49, 279–286.
- Hamidi, M., Kavianpour, M.R. and Shao, Y.P. (2017) A quantitative evaluation of the 3–8 July 2009 Shamal dust storm. *Aeolian Research*, 24, 133–143.
- Jin, Q.J., Wei, J.F. and Yang, Z.L. (2014) Positive response of Indian summer rainfall to Middle East dust. *Geophysical Research Letters*, 41(11), 4068–4074.
- Jin, Q.J., Yang, Z.L. and Wei, J.F. (2016) Seasonal responses of Indian summer monsoon to dust aerosols in the Middle East, India, and China. *Journal of Climate*, 29(17), 6329–6349.
- Lee, Y.G., Kim, J., Ho, C.-H., An, S.-I. and Yeh, S.-W. (2015) The effects of ENSO under negative AO phase on spring dust activity over northern China: an observational investigation. *International Journal of Climatology*, 35, 935–947.
- Li, F., Wang, H.J. and Gao, Y.Q. (2014) On the strengthened relationship between the East Asian winter monsoon and Arctic Oscillation: a comparison of 1950–70 and 1983–2012. *Journal of Climate*, 27(13), 5075–5091.
- Li, Z.X., Yu, Y.Q., Deng, W.T., Zeng, G. and Wu, L.L. (2019) Variation characteristics of North Atlantic tri-polar sea surface temperature in spring and its relationship with NAO and ENSO. *Journal of the Meteorological Sciences*, 039(006), 721–730.
- Liu, J., Wu, D., Liu, G., Mao, R. and Wang, X. (2020) Impact of Arctic amplification on declining spring dust events in East Asia. *Climate Dynamics*, 54, 1913–1935.
- Mao, R., Gong, D.Y., Bao, J.D. and Fan, Y.D. (2011b) Possible influence of Arctic Oscillation on dust storm frequency in North China. *Journal of Geographical Sciences*, 21, 207–218.
- Mao, R., Gong, D.Y. and Fan, Y.D. (2005) Influences of synoptic variability on spring sand storm frequency in North China. *Acta Geographica Sinica*, 01, 12–20.
- Mao, R., Gong, D.Y., Yang, J. and Bao, J.D. (2011c) Linkage between the Arctic Oscillation and winter extreme precipitation over central-southern China. *Climate Research*, 50(2–3), 187–201.
- Mao, R., Ho, C.H., Shao, Y.P., Gong, D.Y. and Kim, J. (2011a) Influence of Arctic Oscillation on dust activity over northeast Asia. *Atmospheric Environment*, 45(2), 326–337.
- Mao, R., Hu, Z.Y., Zhao, C., Gong, D.Y. and Wu, G.J. (2019) The source contributions to the dust over the Tibetan Plateau: a modelling analysis. *Atmospheric Environment*, 214, 16859.
- Najafi, M.S., Sarraf, B.S., Zarrin, A. and Rasouli, A.A. (2017) Climatology of atmospheric circulation patterns of Arabian dust in western Iran. *Environmental Monitoring and Assessment*, 189(9), 473.

- Nakamura, T., Tachibana, Y., Honda, M. and Yamane, S. (2006) Influence of the Northern Hemisphere annular mode on ENSO by modulating westerly wind bursts. *Geophysical Research Letters*, 33(7), L07709.
- Namdari, S., Karimi, N., Sorooshian, A., Mohammadi, G. and Sehatkashani, S. (2018) Impacts of climate and synoptic fluctuations on dust storm activity over the Middle East. *Atmospheric Environment*, 173, 265–276.
- Niranjan Kumar, K., Ouarda, T.B.M.J., Sandeep, S. and Ajayamohan, R.S. (2016) Wintertime precipitation variability over the Arabian Peninsula and its relationship with ENSO in the CAM4 simulations. *Climate Dynamics*, 47(7–8), 2443–2454.
- Plumb R.A. (1985) On the Three-dimensional propagation of stationary waves. *Journal of the Atmospheric Sciences*, 42(3), 217–229. [https://doi.org/10.1175/1520-0469\(1985\)042<0217:ottdpo>2.0.co;2](https://doi.org/10.1175/1520-0469(1985)042<0217:ottdpo>2.0.co;2)
- Qian, Y., Yasunari, T., Doherty, S., Flanner, M. and Zhang, R. (2015) Light-absorbing particles in snow and ice: measurement and modeling of climatic and hydrological impact. *Advances in Atmospheric Sciences*, 32(01), 64–91.
- Rezazadeh, M., Irannejad, P. and Shao, Y.P. (2013) Climatology of the Middle East dust weather frequency. *Aeolian Research*, 10, 103–109.
- Shao, Y.P., Klose, M. and Wyrwoll, K.H. (2013) Recent global dust trend and connections to climate forcing. *Journal of Geophysical Research: Atmospheres*, 118, 11107–11118.
- Shi, L., Zhang, J.H., Yao, F.M., Zhang, D. and Guo, H.D. (2019) Temporal variation of dust emissions in dust sources over Central Asia in recent decades and the climate linkages. *Atmospheric Environment*, 222, 117176.
- Soleimani, Z., Teymouri, P., Boloorani, A.D., Mesdaghinia, A. and Griffin, D.W. (2020) An overview of bioaerosol load and health impacts associated with dust storms: a focus on the Middle East. *Atmospheric Environment*, 223, 117187.
- Song, J., Li, C. and Zhou, W. (2014) High and low latitude types of the downstream influences of the North Atlantic Oscillation. *Climate Dynamics*, 42, 1097–1111.
- Sun, Z.B., An, X.Q., Cui, M.M., Tao, Y. and Ye, C. (2016) The effect of PM<sub>2.5</sub> and PM<sub>10</sub> on cardiovascular and cerebrovascular diseases admission visitors in Beijing areas during dust weather, non-dust weather and haze pollution. *China Environmental Science*, 36(8), 2536–2544.
- Thompson D.W. J., and Wallace J.M. (1998) The Arctic oscillation signature in the wintertime geopotential height and temperature fields. *Geophysical Research Letters*, 25(9), 1297–1300. <https://doi.org/10.1029/98gl00950>
- Türkes, M. and Erlat, E. (2008) Influence of the Arctic Oscillation on the variability of winter mean temperatures in Turkey. *Theoretical and Applied Climatology*, 92(1–2), 75–85.
- Wu, Z., Wang, B., Li, J. and Jin, F. (2009) An empirical seasonal prediction model of the east Asian summer monsoon using ENSO and NAO. *Journal of Geophysical Research*, 114, D18120.
- Zhao, W., Chen, S., Chen, W., Yao, S.-L. and Yu, B. (2019) Inter-annual variations of the rainy season withdrawal of the monsoon transitional zone in China. *Climate Dynamics*, 53, 2031–2046.
- Zhao, W., Chen, W., Chen, S., Yao, S.-L. and Nath, D. (2020) Combined impact of tropical central-eastern Pacific and North Atlantic sea surface temperature on precipitation variation in monsoon transitional zone over China during August–September. *International Journal of Climatology*, 40, 1316–1327.

## SUPPORTING INFORMATION

Additional supporting information may be found in the online version of the article at the publisher's website.

**How to cite this article:** Sun, Y., Mao, R., Gong, D.-Y., Li, Y., Kim, S.-J., Zhang, X.-X., Zhang, X., & Hamidi, M. (2022). Decadal shift of the influence of Arctic Oscillation on dust weather frequency in spring over the Middle East during 1974–2019. *International Journal of Climatology*, 42(4), 2440–2454. <https://doi.org/10.1002/joc.7375>